Available online at www.sciencedirect.com
ScienceDirect
Journal of Nuclear Materials 372 (2008) 226–232
journal of nuclear materials
www.elsevier.com/locate/jnucmat

Plasma-sprayed yttria-stabilized zirconia coatings on type 316L stainless steel for pyrochemical reprocessing plant

A. Ravi Shankar, U. Kamachi Mudali *, Ravikumar Sole, H.S. Khatak, Baldev Raj

Corrosion Science and Technology Division, Indira Gandhi Centre for Atomic Research, Kalpakkam 603 102, India

Received 14 August 2006; accepted 15 March 2007

Abstract

Type 316L stainless steel (SS) is one of the candidate materials proposed for application in pyrochemical reprocessing plants. In the present work, yttria-stabilized zirconia coatings of 300 μm were applied over type 316L SS with a metallic bond coating of 50 μm by an optimized plasma spray process, and were assessed for the corrosion behaviour in molten LiCl–KCl medium at 873 K for periods of 5 h, 100 h, 250 h and 500 h. The as-coated and tested samples were examined by optical microscopy and SEM for homogeneity, penetration of molten salt through coating and corrosion of type 316L SS substrate. The results indicated that the yttria-stabilized zirconia coatings performed well without significant degradation and corrosion attack. Laser melting of the coated samples using CO_2 laser was attempted to consolidate the coatings. The development of large grains with segmented cracks was noticed after laser melting, though the coating defects have been eliminated.

1. Introduction

A sodium cooled fast reactor cycle system with metallic fuel has been chosen as the best option for the future Indian fast breeder reactors [1]. For reprocessing of spent metallic fuels, a metallic electrorefining method and a fuel fabrication system with a metal injection casting method have been chosen as the promising candidate concepts [2]. A pyrometallurgical nuclear fuel recycle process, called pyroprocess, has originally been developed by Argonne National Laboratory (ANL) [3]. In the early 1980s, the studies on the electro-deposition of uranium at solid cathodes have been conducted at ANL towards the integrated fast reactor fuel processing program [4]. The Russian RIAR (Research Institute of Atomic Reactors) process was also related to the pyroelectrochemical processes for recycling of irradiated fast reactor oxide fuels [5]. The electrorefining process was carried out in an electrorefiner that contains a molten chloride salt (LiCl–KCl) floating on liquid cadmium operating at 773 K under an argon atmosphere [3]. The sheared spent fuel charged in anode baskets of the electrorefiner was refined in the molten salt while uranium was recovered at a solid cathode and U–Pu–MA (minor actinides) were collected at a liquid cadmium cathode [2]. Corrosion resistance of the materials in molten chloride salts at high temperature is of prime importance for equipments like electrorefiner and salt purification vessel in pyrochemical reprocessing plants.

Molten salts can cause corrosion to container materials and other accessories used in the construction of various equipments. Corrosion studies were carried out by Indacochea et al. [6] on type 316L stainless steel (SS), type 422 SS, type 430 SS, 2.25 Cr–1 Mo steel, and Ta in annealed and welded conditions, in LiCl molten salt with 3.5 wt% Li_2O, 1 wt% Li_3N at 998 K for 30 days. These ferrous alloys and Ta did not show significant weight change or corrosion attack under reducing conditions after 30 days of exposure [6]. This suggested that 316L SS could be one of the suitable material, where molten LiCl–KCl salts were utilised. The ceramic materials like ZrO_2, ZrO_2–SiO_2, and pyrolitic graphite are promising for severe molten salt corrosion environments, particularly for fuel

* Corresponding author. Tel.: +91 44 27480121; fax: +91 44 27480301.
E-mail address: kamachi@igcar.gov.in (U. Kamachi Mudali).

0022-3115/$ - see front matter © 2007 Elsevier B.V. All rights reserved.
doi:10.1016/j.jnucmat.2007.03.175

reprocessing by the RIAR process [7]. Thermodynamic stabilities of various ceramic materials like oxides, carbides, nitrides, etc. indicated a better stability of ZrO_2 in highly corrosive environments like Cl_2, O_2, and $UO_2Cl_2 + Cl_2$ [7,8]. The corrosion resistance of ZrO_2 ceramic in molten NaCl–KCl salt under Cl_2 bubbling at 1023 K for 24 h was about 0.5 mm/yr [8]. It is well known that zirconia-stabilized with 6–8 wt% yttria coatings exhibited the maximum thermal cycle life [9].

Based on the literature, coating of 7–9 wt% yttria-stabilized zirconia on type 316L SS has been choosen as one of the candidate materials for the salt purification vessel and electrorefiner. The plasma spray process was considered as the economical method of producing reproducible and durable thick zirconia coatings of thermal barrier type, and this has been widely used in the aerospace industry. Hence, plasma spray zirconia coatings applied over type 316L SS have been chosen for corrosion investigations in a molten chloride medium. The present paper also investigates laser melting as a possible step to consolidate the plasma-sprayed zirconia coatings.

2. Experimental work

2.1. Materials and coating

The chemical composition of AISI type 316L SS used for the present investigation is given in Table 1. Type 316L SS rods 100 mm long and 5 mm diameter in pickled and passivated condition were used. The passivated rods were then coated with a two-layer thermal barrier coating with the first layer by vacuum plasma-sprayed NiCrAlY which acts as a bond coat, followed by a top coat of yttria-stabilized (≈8 wt%) zirconia coating. The air plasma-sprayed zirconia layer acts as a corrosion resistant thermal barrier. The coated layers were produced by M/s Plasma Spray Processors, Mumbai by using a METCO 9 MB type plasma gun. The bond coat was 50 μm thick whilst the ceramic zirconia top coat was 300 μm thick. The composition of the ceramic powder used was Y_2O_3 (7–9 wt%)–SiO_2 (1 wt%)–TiO_2 (0.2 wt%)–Al_2O_3 (0.2 wt%)–Fe_2O_3 (0.2 wt%)–ZrO_2 (balance). The particle sizes of bond coat and ceramic coat powders were between (250 ± 50) μm and (80 ± 20) μm, respectively. The optimized spray parameters employed for plasma coating are given in Table 2.

2.2. Corrosion testing in molten salt

LiCl–KCl salts are highly hygroscopic in nature, hence all the operations have been carried out in an argon atmosphere containing glove box. In the present investigation, corrosion tests were carried out in a molten salt test assembly (MOSTA) specifically designed and fabricated for corrosion testing of coated samples in molten LiCl–KCl salt. The schematic diagram of the furnace used for the corrosion studies is shown in Fig. 1. The salt used has a eutectic composition of LiCl (44.48 wt%) and KCl (55.52 wt%) with a melting point of 634 K. The stainless steel cell along with the sample was initially taken into an argon atmosphere glove box. The salt was loaded in the alumina crucible and placed in the stainless steel cell, along with sample and thermocouple in right position. The cell was sealed inside the glove box and taken out for connecting with the argon lines of the furnace. The tests were carried out at a temperature of 873 K for 5 h, 100 h, 250 h and 500 h

Table 2
Plasma spray parameters for coating of partially stabilized zirconia over type 316L SS

Plasma spraying equipment	METCO 9 MB type
Voltage	64–70 V
Current	600 A
Arc gases, primary	Ar
secondary	H_2
Powder feed rate	2.75 kg h^{-1}
Powder carrier gas	Ar
Stand-off distance	100 mm
Flame temperature	11273 K
Velocity of particles	$\leqslant$549 m s^{-1}
Cooling of substrate	Air blowing

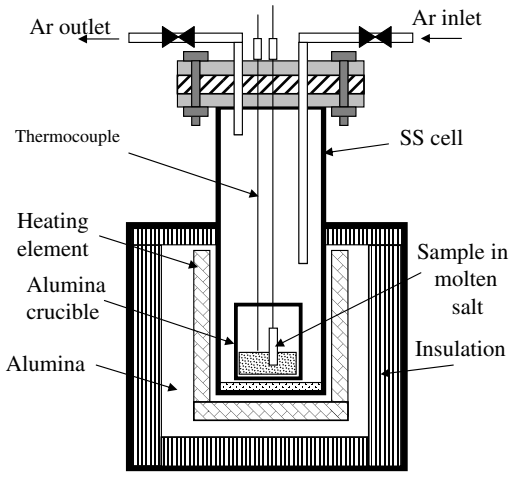

Fig. 1. Schematic diagram of furnace for testing coatings using molten salt test assembly (MOSTA).

Table 1
Chemical composition of type 316L SS (in wt%)

Material	Fe	Cr	Ni	Mo	Si	Mn	S	P	C	N
316L SS	Balance	17.9	12.1	2.45	0.98	1.76	0.002	0.026	0.025	0.068

with continuous argon purging through out the experiment. Before and after the test, the samples were ultrasonically cleaned in acetone. Initial weight and final weight of the samples exposed to the molten salt were taken to assess the extent of corrosion. After the tests, the corroded samples were cut by a diamond cutter and ultrasonically cleaned in acetone for characterization purposes.

2.3. Characterization of samples

The as-coated sample was characterized for porosity and surface morphology by optical microscopy. The area percentage porosity of coatings has been done using ASTM E 2109, by following method A, and involving direct manual comparison with seven standard images [10]. The microhardness measurements were made along the cross-section using a SHIMADZU HMV-2 microhardness tester at 100 g load. The surface of the as-coated and tested samples were examined using scanning electron microscopy (SEM) to assess the degradation of the coating after exposure to molten salt. The cross- sections of the samples exposed to molten salt were examined by optical microscopy to examine the penetration of molten salt through the pores and cracks and subsequent corrosion, if any.

2.4. Laser treatment for consolidation of coating

The coated samples were laser treated at 50 and 100 W power using a 500 W CO_2 continuous wave (CW) laser (wave length 10.64 μm) with a 3-axis computer numerical controller (CNC) workstation, in order to consolidate the coating to produce smooth surface and for eliminating pores and cracks. Laser beam having 1.5 mm beam dia with a raster speed of 2500 μm/s was scanned over an area of 1.5 cm × 2.5 cm with a step size of 500 μm. The laser treated samples were characterized by optical microscopy and SEM to observe the microstructural changes produced after laser melting. X-ray diffraction (XRD) studies were also carried out using a Philips X'pert MPD system (40 kV, 30 mA, Cu Kα_1 radiation at 154.056 pm) to examine the phases present before and after laser treatment. A 2θ scanning rate of $0.02^\circ\ s^{-1}$ was used to determine the peak positions of the phases in the range $20^\circ < 2\theta < 80^\circ$.

3. Results and discussion

3.1. Physical characterization of coating

Partially stabilized zirconia as thermal barrier coatings by the plasma spray process has been extensively studied for gas turbine engine applications as they exhibited good thermal cycling resistance. The plasma-sprayed thermal barrier coatings usually contain up to 10% porosity. Porosity is an important parameter which determines various properties of TBC's like thermal shock and thermal cycling resistance [11]. Area percentage porosity measured by following ASTM E 2109 indicated the porosity of the coatings around 10%. The cross-section microhardness indicated fairly high hardness values ($H_v = 1100$) in the ceramic region, a hardness value of $H_v = 249$ in the bond coat region, and a hardness value of $H_v = 283$ in the substrate, as indicated in Fig. 2. During plasma spraying ceramic powders are melted and rapidly solidified over the substrate as individual splats [11]. The SEM micrograph of an as-coated surface showed porosity and typical individual splats as shown in Fig. 3(a).

3.2. Corrosion investigations in molten LiCl–KCl salt

The coated samples were exposed to molten LiCl–KCl salt with continuous argon purging for various durations. The percentage weight loss of the samples exposed for 100 h and 500 h was about 0.3%. This indicated better corrosion resistance of ZrO_2 in molten LiCl–KCl. The important factors in molten salt corrosion are impurities, defects, heterogeneities of the material and also the chemical nature of the oxidant involved in the liquid. The corrosion reaction in molten salts is a fairly complex phenomenon compared to an aqueous medium [12].

The corrosion of metals and alloys in molten chlorides has been attributed mostly to the presence of trace impurities like moisture, water and oxygen present in the salt [6]. Metals and alloys can corrode owing to a trace of water or moisture in molten chlorides, even in the absence of oxygen. The corrosion reaction in molten salts can be expressed by the partial anodic reaction and partial cathodic reduction of the oxidant. In molten salts, there are

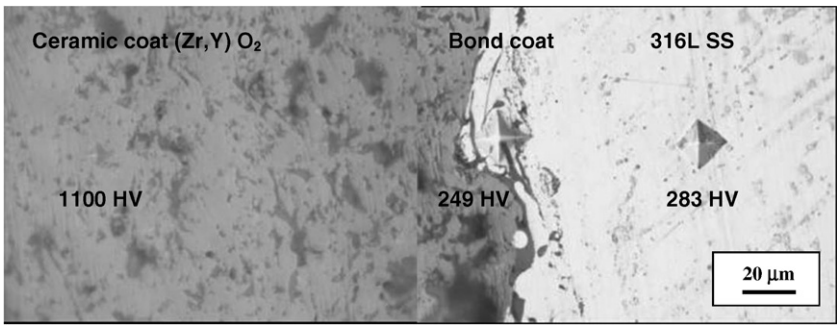

Fig. 2. The cross-section microstructure of partially stabilized zirconia coated over type 316L SS with a bond coat (also showing the microhardness).

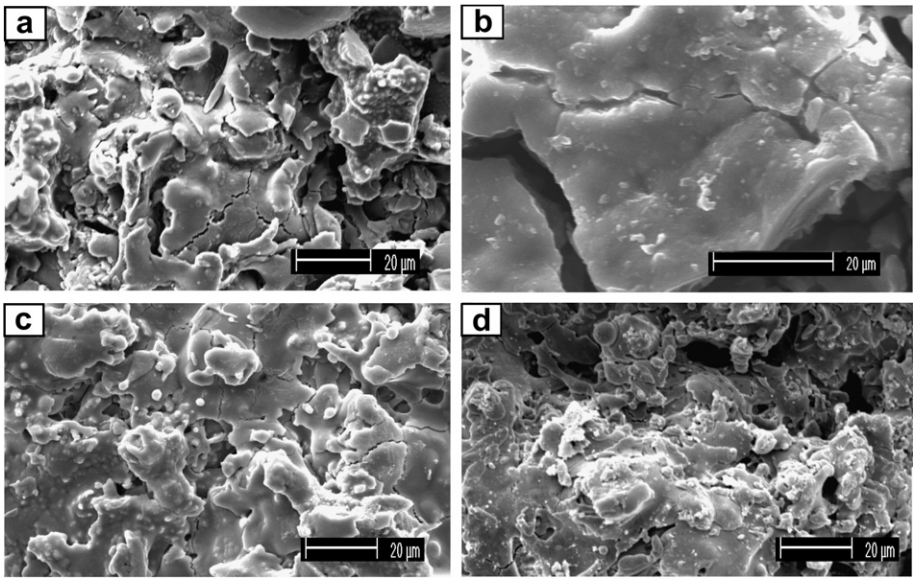

Fig. 3. SEM micrographs of partially stabilized zirconia coated over type 316L SS in: (a) as-coated, (b) 5 h exposed, (c) 100 h exposed and (d) 500 h exposed to molten LiCl–KCl salt.

several oxidants (O_2, H^+, H_2O and OH^-) common to the molten salts, and such oxidants are associated with the dissociation reaction of molten salts themselves [12]. According to Nishikata et al. [12] the reactions involved during molten salt corrosion are as follows.

The partial anodic reactions for metals and alloys are

$$M \rightarrow M^{n+} + ne^-$$

$$M^{n+} + 1/2nO^{2-} \rightarrow MO_{n/2}$$

The partial reduction reactions due to the oxidants are

$$O_x + ne^- \rightarrow R$$

where O_x and R represent oxidant and reductant, respectively, and n is the number of electrons involved,

$$H_2O + e^- \rightarrow 1/2H_2 + OH^-$$

$$OH^- + e^- \rightarrow 1/2H_2 + O^{2-}$$

$$H^+ + e^- \rightarrow 1/2H_2$$

$$O_2 + 2e^- \rightarrow O_2^{2-}$$

$$O_2 + 2H_2O + 4e^- \rightarrow 4OH^-$$

Critical vapour pressure values of the metal chlorides are often used to assess the resistance of different materials to chlorides [13]. In zirconia, coating impurities like SiO_2, TiO_2, Al_2O_3 and Fe_2O_3 are present in small quantities, and the temperatures of such chlorides at the critical vapour pressure (10^{-4} bar) where they would evaporate are −235 K ($TiCl_4$), 349 K ($AlCl_3$), and 440 K ($FeCl_3$) [13]. Hence significant evaporation of these metal chlorides may occur when the components operate at high temperatures. Indeed, in the present work evaporation and deposition of salts over the surface of the alloy/coating above the molten salt level have been observed. The sample exposed for 5 h exhibited clear salt deposits over the surface (Fig. 3(b)). The vapour-exposed region of the 250 h and 500 h samples also showed faceted deposits containing salt crystals typically around 1 μm sizes as shown in Fig. 4. Such deposits were observed all along the vapour-exposed region of all tested samples. The EDX analysis of the 5 h and 100 h exposed samples were shown in Fig. 5. The EDX analysis of the 100 h exposed sample revealed the peak of Zr, while that of the 5 h exposed sample indicated

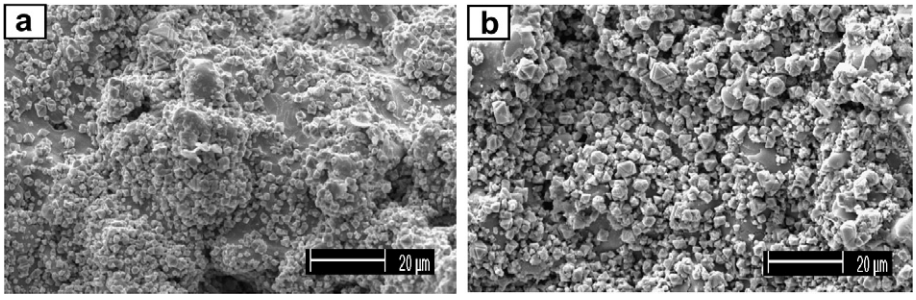

Fig. 4. SEM micrographs of partially stabilized zirconia coated over type 316L SS from the vapour-exposed portion of the samples showing salt deposition in both (a) 250 h exposed, (b) 500 h exposed to molten LiCl–KCl salt.

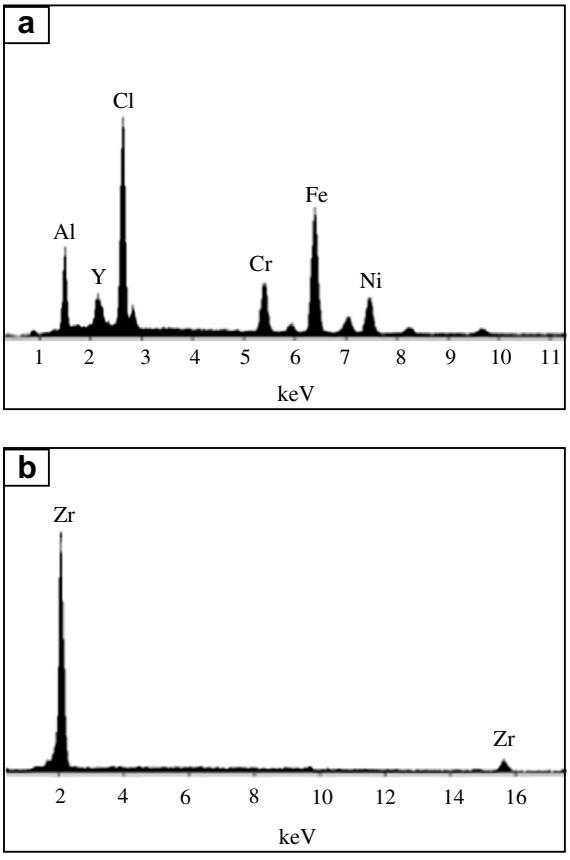

Fig. 5. EDX from (a) 5 h exposed, and (b) 100 h exposed sample.

peaks close to Fe, Cr, Ni, Al and major Cl peaks. The molten chloride species in the uncoated area react with the underlying metal/oxide and volatile metal chlorides form due to low temperature of vapourisation. Haanappel et al. [14] have schematically described the possible reactions in an oxygen- and chlorine-containing environment similar to the scheme shown below:

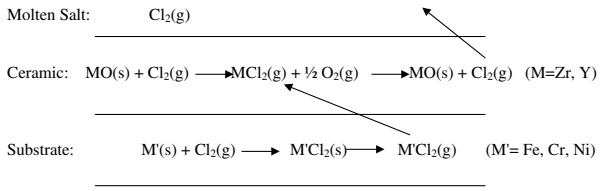

The particles attain the molten state and rapidly solidify during plasma spraying however, shrinkage and differential thermal stresses produced microcracks as seen in Fig. 3(a). In the present study, however, except for the sample exposed to LiCl–KCl for 5 h, the SEM micrograph of the 100 h, 250 h and 500 h exposed samples are similar in appearance to that of the as-coated surface (Fig. 3(c) and (d)). The surface of such samples showed little or no degradation of the coating after exposure to molten salt up to 500 h.

3.3. Effect of laser melting

Laser treatment of ceramic coatings provides a better coating structure, and reduced porosity, which in turn offers a positive influence on the mechanical and corrosion properties of coatings [15]. The presence of porosity and microcracks as observed for the coated specimen shown in Fig. 3(a), would cause the penetration of salt and subsequent corrosion of the substrate over long periods of service. The cross-section of the molten salt exposed samples up to 500 h, did not reveal the penetration of molten salts through the pores and subsequent corrosion of the substrate. However, in order to eliminate the porosity and cracks, and to produce a smooth surface, laser melting was carried out at 50 and 100 W. The melted glossy surface was initially observed by optical microscopy, which revealed cellular grains of zirconia as shown in Fig. 6.

SEM micrographs of the laser-melted surface at 50 and 100 W became smooth (Fig. 7(a) and (b)) as compared to the rough as-coated surface on the left-hand side of Fig. 7(a). The interface of the laser-melted and as-coated surface is shown in Fig. 7(a) where a network of cracks has been clearly seen in the melted portion. At higher magnifications, these cracks were found to decorate all along the grain boundaries. These segmented cracks could have formed due to shrinkage and differential thermal stresses arising during rapid solidification on laser melting [16]. It has been reported that zirconia coatings containing ≈8 wt% Y_2O_3 prepared by plasma spraying or laser treatment produced metastable tetragonal (t′) phase because of rapid solidification and subsequent cooling [17,18]. The presence of the tetragonal (t′) phase in thermal barrier coatings was expected to be highly beneficial because of its thermal stability [9] and structural hardening [17]. It has also been reported that the tetragonal phase gives split peaks while cubic does not [18]. The (200), (113) and (400) split peaks of the tetragonal phase in the XRD patterns of the 50 and 100 W laser-melted surfaces indicated the presence of higher amounts of the tetragonal phase in

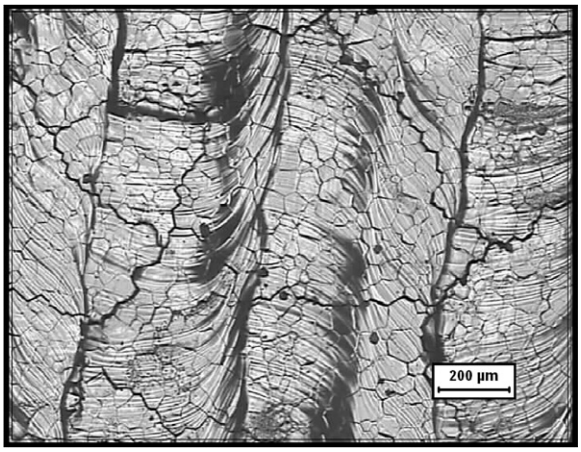

Fig. 6. Optical micrograph of laser-melted partially stabilized zirconia coating over type 316L SS at 100 W power.

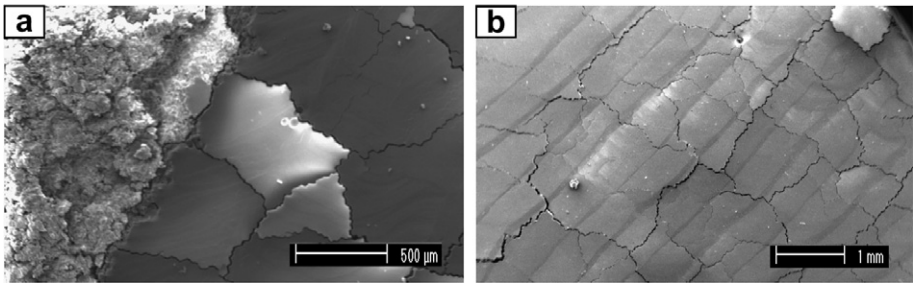

Fig. 7. SEM micrographs of partially stabilized zirconia coating over type 316L SS laser-melted at (a) 50 W and (b) 100 W.

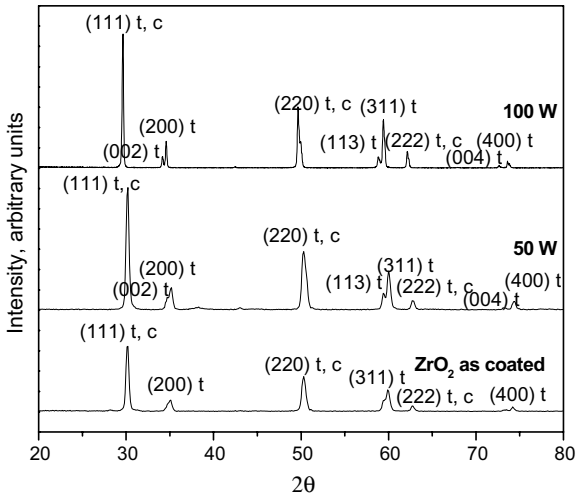

Fig. 8. XRD patterns of as-coated and laser-melted partially stabilized zirconia coating over type 316L SS.

addition to cubic phases in the laser-melted sample (Fig. 8). This is in agreement with the results reported by Wang et al. [18]. Indeed, the 100 W laser-melted surface indicated more distinctive (2 0 0), (1 1 3) peaks of the tetragonal phase split in comparison with the 50 W laser-melted surface. However, the presence of metastable tetragonal (t′) phase has to be confirmed by slow scanning in the range 72–90° during XRD study. The cross-sections of the as-coated and laser-melted samples were also observed in order to determine the track width and depth of the laser-melted region. The laser parameters need to be optimized to obtain a smooth surface without cracks in order to provide good corrosion resistance in molten salt environment.

4. Conclusions

It was found from the immersion experiments performed up to 500 h at 873 K in molten LiCl–KCl that the yttria-stabilized zirconia coating over type 316L SS exhibited good corrosion resistance. Weight loss experiments indicated insignificant weight change after immersion up to 500 h. Microstructural examination of the tested samples using optical microscopy and SEM did not reveal any significant degradation over the surface, and no penetration of salt across the coating to attack the substrate. The sample exposed for 5 h and vapour-exposed region of samples tested for 250 and 500 h exhibited salt deposits. Laser consolidation of zirconia coatings resulted in smooth surface as against porous and cracked as-coated plasma-sprayed surface. Laser-melting also eliminated porosity and revealed well delineated grains of zirconia as observed from optical and SEM microscopy. Segmented crack network along grain boundaries in laser treated samples are due to shrinkage and relief of thermal stresses which need to be controlled by optimizing the laser parameters. X-ray diffraction patterns indicated the presence of higher amounts of the tetragonal phase in laser-melted samples. Further work is in progress for the corrosion evaluation at longer durations, and to optimize laser parameters for the consolidation of coatings.

Acknowledgements

The authors would like to acknowledge Dr B. Prabhakara Reddy, Chemistry Group, for preparing the salt, and Sri. M. Arumugam of CSTD, for fabrication and operation of the molten salt test assembly (MOSTA). The authors would also like to acknowledge Smt. M. Radhika for SEM examination of the samples.

References

[1] Baldev Raj, H.S. Kamath, R. Natarajan, P.R. Vasudeva Rao, Prog. Nucl. Energ. 47 (2005) 369.
[2] K. Sato, T. Fujioka, H. Nakabayashi, S. Kitajima, T. Yokoo, T. Inoue, in: Proceedings of Global 2003, New Orleans, November 16–20, 2003, p. 744.
[3] T. Koyama, M. Iizuka, Y. Shoji, R. Fujita, H. Tanaka, T. Kobayashi, M. Tokiwai, J. Nucl. Sci. Technol. 34 (1997) 384.
[4] J.L. Willit, W.E. Miller, J.E. Battles, J. Nucl. Mater. 195 (1992) 229.
[5] M.V. Kormilitsyn, A.V. Bychkov, V.S. Ishunin, in: Proceedings of Global 2003, New Orleans, November 16–20, 2003, p. 782.
[6] J.E. Indacochea, J.L. Smith, K.R. Litko, E.J. Karell, J. Mater. Res. 14 (1999) 1990.
[7] M. Asou, S. Tamura, T. Namba, H. Kamoshida, Y. Shoji, K. Mizuguchi, T. Kobayashi, in: Proceedings of Global 1999, Jackson Hole, Wyoming, August 29–September 3, 1999.
[8] M. Takeuchi, T. Kato, K. Hanada, T. Koizumi, S. Aose, J. Phys. Chem. Solids 66 (2005) 521.
[9] Kurt H. Stern, Metallurgical and Ceramic Protective Coatings, Chapman & Hall, UK, 1996.

[10] ASTM E 2109-00, Test methods for determining area percentage porosity in thermal sprayed coatings.
[11] J.R. Davis, Davis & AssociatesMicrostructural Characterization of Thermal Spray Coatings, vol. 9, ASM Handbook, Materials Park, Ohio, 2004.
[12] A. Nishikata, H. Numata, T. Tsuru, Mater. Sci. Eng. A 146 (1991) 15.
[13] Michael Schutze, Corrosion and Environmental Degradation, vol. 1, Wiley-VCH, Weinheim, 2000.
[14] V.A.C. Haanappel, T. Fransent, P.J. Gellings, High Temp. Mater. Proc. 10 (1992) 67.
[15] A. Pokhmurska, R. Ciach, Surf. Coat. Technol. 125 (2000) 415.
[16] A. Petitbon, L. Boquet, D. Delsart, Surf. Coat. Technol. 49 (1991) 57.
[17] G. Antou, G. Montavon, F. Hlawka, A. Cornet, C. Coddet, F. Machi, Surf. Coat. Technol. 172 (2003) 279.
[18] X. Wang, P. Xiao, M. Schmidt, L. Li, Surf. Coat. Technol. 187 (2004) 370.